

Elastic $\pi - N$ scattering in the $I = 3/2$ channel

Constantia Alexandrou,^{a,b} Kyriakos Hadjiannakou,^{a,b} Giannis Koutsou,^b Srijit Paul,^c Ferenc Pittler,^{b,*} Marcus Petschlies^d and Antonino Todaro^{a,d,e}

^a*Department of Physics, University of Cyprus, 20537 Nicosia, Cyprus*

^b*Computation-based Science and Technology Research Center, The Cyprus Institute, Cyprus*

^c*Institut für Kernphysik, Johannes Gutenberg-Universität Mainz, 55099 Mainz, Germany*

^d*HISKP (Theory), Rheinische Friedrich-Wilhelms-Universität Bonn, Germany*

^e*Dipartimento di Fisica and INFN, Università di Roma "Tor Vergata", I-00133 Rome, Italy*

^f*Institut für Physik, Humboldt-Universität zu Berlin, Newtonstrasse 15, 12489 Berlin, Germany*

E-mail: f.pittler@cyi.ac.cy

We present our study of $\pi - N$ scattering in the iso-spin $I = 3/2$ channel for the first time at the physical point. The calculation is performed using $N_f = 2 + 1 + 1$ flavors of twisted mass fermions with clover improvement at physical pion mass. We compute energy levels for the rest frame and moving frames up to a total momentum of $|\vec{P}| = \sqrt{3} \frac{2\pi}{L}$, and for all the relevant irreducible representations of the lattice symmetry groups. We perform a phase-shift analysis including $s(\ell = 0)$ and $p(\ell = 1)$ wave phase shifts assuming a Breit-Wigner form and determine the parameters of the Δ resonance.

*The 38th International Symposium on Lattice Field Theory, LATTICE2021 26th-30th July, 2021
Zoom/Gather@Massachusetts Institute of Technology*

*Speaker

1. Introduction

The study of resonances with lattice methods in Euclidean field theory has matured from the initial proposal by Lüscher [2] to deploy the finite volume as a probe for scattering properties of hadrons. A prime example that speaks to these current capabilities are the numerous studies of meson-meson scattering, and in particular of the $\rho(770)$ meson. Determinations of ρ resonance parameters have been carried out by a number of lattice QCD collaborations. More recently, lattice calculations of the ρ have been advanced even to the point of physical pion mass [3–7].

With meson-baryon scattering the situation is less advanced by comparison. A natural step is the study of the simplest resonance in pion-nucleon ($\pi - N$) scattering, namely the well-known $\Delta(1232)$. Moreover, with presently available gauge configurations we can approach elastic $\pi - N$ scattering at physical pion mass, with realistic comparison to experimental results. This is the topic of our contribution. The Δ is the lightest baryon spin-3/2 resonance. It is well isolated from other resonances and decays almost exclusively to $\pi - N$. The decay $\Delta \rightarrow N\gamma$ corresponds to less than 1% of the total decay width. Besides the theoretical interest, the presence of Δ in compact neutron stars makes it important for phenomenology as well. The interaction between Δ and nucleon could generate thermodynamic instabilities in compact neutron stars [8].

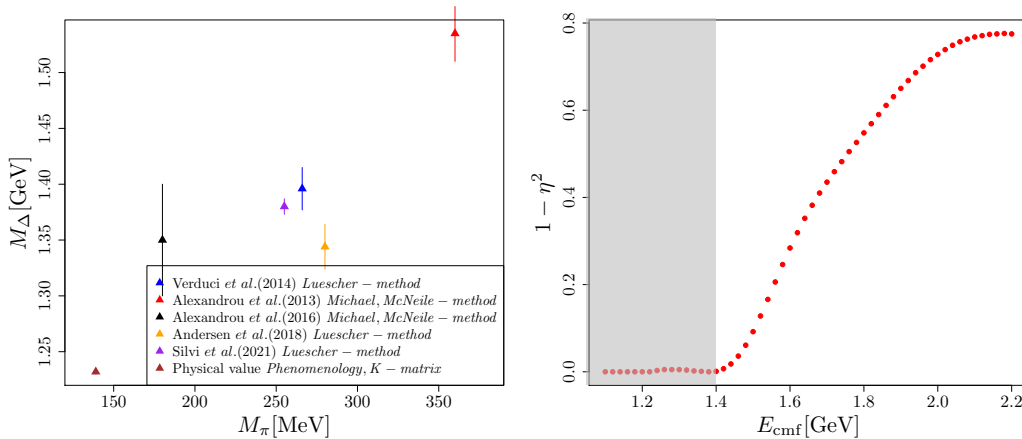


Figure 1: Left: Previous determinations of the Δ -resonance mass as function of the pion mass. In italics we give the method which is used in the computation. Right: The inelasticity of the scattering in the Δ channel, shaded gray area shows the energy range considered in this work. Data is taken from [12].

With the left-hand plot in Fig. 1 we briefly comment on already available lattice studies of the Δ and its coupling to the $\pi - N$ state. Two different type of methods were previously used to study Δ resonance parameters: the Lüscher approach mentioned above and denoted as *Luescher-method* in the legend, and the transfer matrix approach introduced in Ref. [9] denoted as *Michael, McNeile-method*. However, the latter method assumes a quasi-stable Δ state perturbatively close in mass to $\pi - N$ threshold, to extract the $\Delta - N\pi$ transition matrix element and the coupling. At this early stage the displayed individual studies given by the

ensemble	M_π/MeV	M_N/MeV	$M_\pi L$	a/fm	N_{conf}	N_{src}
cB211.072.64	139.43(9)	944(10)	3.622(3)	0.0801(2)	388	64

Table 1: Parameters of the ensemble used in this work; further details are given in Ref. [10]. The right-most columns give the number of gauge configurations employed N_{conf} and the number of point sources used per configuration N_{src} .

pion mass, at which they were carried out, differ completely by lattice action, type and size of discretization artifacts and finite-volume effects. We report on our Lüscher-method based $\pi - N$ elastic scattering analysis in the Δ channel, for the first time directly at physical pion mass and with strange and charm quark close to their physical values. This setup provides us with the well-known numeric difficulty of fast exponential deterioration of the signal-to-noise ratio in (meson-)baryon correlators and given the low pion mass only a small energy range of the $\pi - N$ system for elastic scattering $E_{2,\text{thr}} = m_N + m_\pi \leq \sqrt{s} \leq m_N + 2m_\pi = E_{3,\text{thr}}$, between 2- and 3-particle threshold, where the 2-particle quantization condition is rigorously applicable. However, we take the SAID inelasticity data [12] shown in the right-hand plot of Fig. 1 as indication, that p -wave $\pi - N$ scattering can be treated as elastic up to $\sqrt{s} = 1.4$ GeV.

2. Simulation details

In our simulation setup we use $N_f = 2 + 1 + 1$ flavors of twisted-clover fermions with physical quark masses from the Extended Twisted Mass Collaboration (ETMC). The important ensemble properties regarding this work are summarized in Table 1. More detailed description is given in Ref. [10].

As an input for the Lüscher analysis we determine the spectrum of the $\pi - N$ system in the $I = 3/2$ channel from correlation functions of single- (Δ -like) and 2-hadron (πN) interpolators

$$C_{XY}(\vec{p}, t) = \langle O_X^{\vec{p}}(t) \bar{O}_Y^{\vec{p}}(0) \rangle, \quad X, Y \in \{\Delta, \pi N\},$$

with total momentum (and individual particle momenta) up to $|\vec{p}| = \sqrt{3} \frac{2\pi}{L}$. We use the standard interpolating operators for the Δ at maximal $I_3 = +3/2$, the π^+ and proton N given by:

$$O_{\Delta,\mu} = \varepsilon_{abc} \left(u^a C \gamma_\mu u^b \right) u^c, \quad O_\pi = \bar{d} \gamma_5 u, \quad O_N = \varepsilon_{abc} \left(u^{at} C \gamma_5 d^b \right) u^c \quad (1)$$

For the $\pi - N$ 2-hadron interpolator we use the product of the single hadron interpolators π and N . Here we only briefly review our method for calculating two hadron two-point functions. For further details we refer to Ref. [13]. Describing the propagation from source to sink we use point source propagators and in the case of the two-hadrons we use the sequential source technique. The sink to sink propagation is replaced in the πN to πN correlation functions by fully time diluted stochastic source/propagator pairs, along which we cut the diagrams into reusable “factors”. For the latter we implemented GPU-kernels,

Table 2: Momentum frames and irreducible representations used in this work. Second column (ℓ) indicates the infinite volume partial waves contributing to the irreducible representation. In the third column we show the size of the 2d matrix used in the GEVP for the particular irrep.

$\vec{p}_{tot}/(2\pi/L)$	Λ	ℓ	N_{dim}
(0, 0, 0)	G1u	s, \dots	8x8
(0, 0, 0)	Hg	p, f, \dots	9x9
(0, 0, 1)	G1	s, p, d, \dots	24x24
(0, 0, 1)	G2	p, d, \dots	18x18
(1, 1, 0)	(2)G	s, p, d, \dots	30x30
(1, 1, 1)	(3)G	s, p, d, \dots	16x16
(1, 1, 1)	F1	p, d, \dots	6x6
(1, 1, 1)	F2	p, d, \dots	6x6

which reduce 2- and 3-fold propagator products, including momentum projection. All propagators receive Gaussian smearing at source and sink, with $N_G = 140$ smearing steps and weight $\alpha_G = 0.5$, with APE smeared gauge field in the Gaussian smearing kernel with $N_{APE} = 60$, $\alpha_{APE} = 0.5$.

In discretized and finite volume we project interpolating operators to the irreducible representations (irreps Λ with rows μ) of the lattice rotation group 2O_h in the rest frame of the $\pi - N$ system, and the irreps of its subgroups in moving frames with total momentum \vec{p}_{tot} (little groups $LG(\vec{p}_{tot})$). The subduction coefficients U for the group projection of correlators

$$C_{\mathcal{A}_{\text{sink}}, \mathcal{A}_{\text{source}}}^{\Lambda, \beta, \mu, \vec{p}_{tot}} = \sum_{\mathcal{B}_{\text{sink}}, \mathcal{B}_{\text{source}}} U_{\mathcal{B}_{\text{sink}}}^{\star, \beta \mu o_{\text{sink}}} U_{\mathcal{B}_{\text{source}}}^{\beta \mu o_{\text{source}}} C_{\mathcal{B}_{\text{sink}} \mathcal{B}_{\text{source}}} \quad (2)$$

with compound indices $\mathcal{B} = \{\vec{p}_\pi, \vec{p}_N, \alpha\}$ for particle momenta and irrep occurrence, are determined based on [14] with a Gram-Schmidt decomposition for multiple occurrences. The sum at the source and sink is restricted to have a fixed momentum amplitude i.e. $\mathcal{A} = \{|\vec{p}_\pi^2, |\vec{p}_N^2, o\}$. To obtain the first few energy levels we solve the generalized eigenvalue problem (GEVP) for the correlation matrix ($C^{\Lambda, \beta=0, \mu, \vec{p}_{tot}}$) and fit the resulting eigenstates with a single exponential decay:

$$C_{ij}^{\Lambda, \mu, \vec{p}_{tot}}(t) u_j^n(t) = \lambda^n(t, t_0) C_{ij}^{\Lambda, \mu, \vec{p}_{tot}}(t_0) u_j^n(t_0) \quad (3)$$

$$\lambda^n(t, t_0) \propto e^{-E_n(t-t_0)}. \quad (4)$$

We summarize in Table 2 the momenta and irreps used in this work together with the dominant partial waves the given irreps contribute to, and the size of the correlation matrix used in the GEVP analysis.

3. Determining the interacting spectrum

The interaction in the spectrum shows up as a resulting shift of the energy levels with respect to the non-interacting ones. The energy shift is determined from a GEVP. The basis for the GEVP were selected by requiring a stable behavior of the effective mass under removing/changing a few basis vectors. An example for the basis selection we show on the left plot of Fig. 2. We extract the energy levels using single state fits to the principal correlators. We choose t_{\min} by requiring agreement between single and two-states fits and stability by increasing or decreasing t_{\min} by one in lattice units. An example for the stability we show on the right panel of Fig. 2. the results from single and two-state fits.

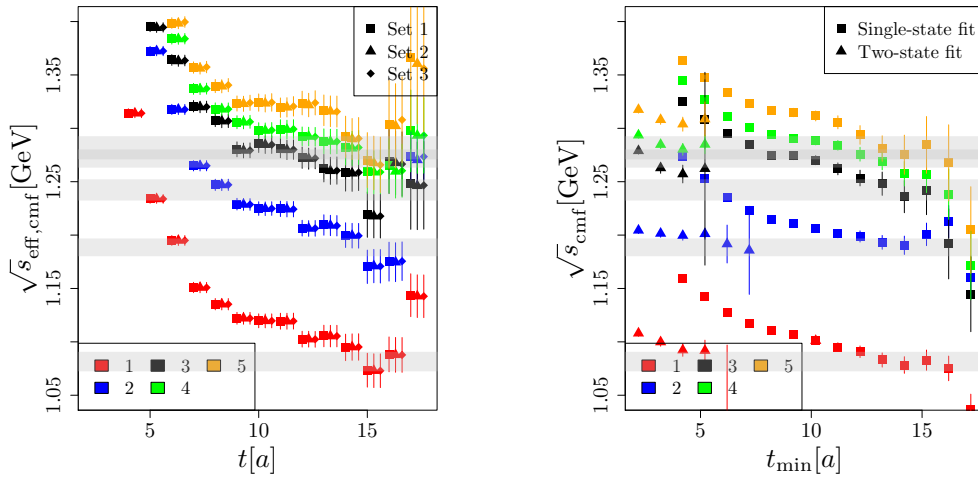


Figure 2: Example for GEVP results in irrep G_1 of the little group $2C_{4v}$. Left: The dependence of the principal correlator effective mass on the basis for the GEVP. Set 1 consists of interpolators from all available momentum configurations and occurrences, Set 1 = $\{\Delta_{1-4}; \pi_1 N_0|_{1-2}; \pi_0 N_1|_{1-2}; \pi_2 N_1|_{1-4}; \pi_1 N_2|_{1-4}; \pi_3 N_2|_{1-4}; \pi_2 N_3|_{1-4}\}$, where the subscript denotes particle momentum and occurrences $|\vec{p}|/(2\pi/L) |1 - \dots$. In Set 2 we take into account half of the occurrences from Set 1 using the signal quality for selection criteria. In Set 3 we have replaced the two occurrences from Set 2 from momentum combinations $\pi_2 N_3$ and $\pi_3 N_2$ with the other two in Set 1. Right: Stability of single and two states fits to the principal correlators as a function of t_{\min} . Gray bands are representing the final fit results from the chosen fit range.

Our results for the interacting spectrum are shown in Fig. 3. As an input for the Lüscher-analysis we restrict the energy window to be below 1.3 GeV, in order to keep contamination from inelastic scattering small.

4. Phase shift analysis

The connection between the finite volume two-particle interacting spectrum and the infinite-volume resonance parameters is encoded in the Lüscher quantization conditions (LQC-s). Mathematically, they are determinant equations given by

$$\det (M_{J\ell n, J'\ell' n'}^\Lambda(s) - \delta_{JJ'} \delta_{\ell\ell'} \delta_{nn'} \cot\delta_{J\ell}(s)) = 0, \quad (5)$$

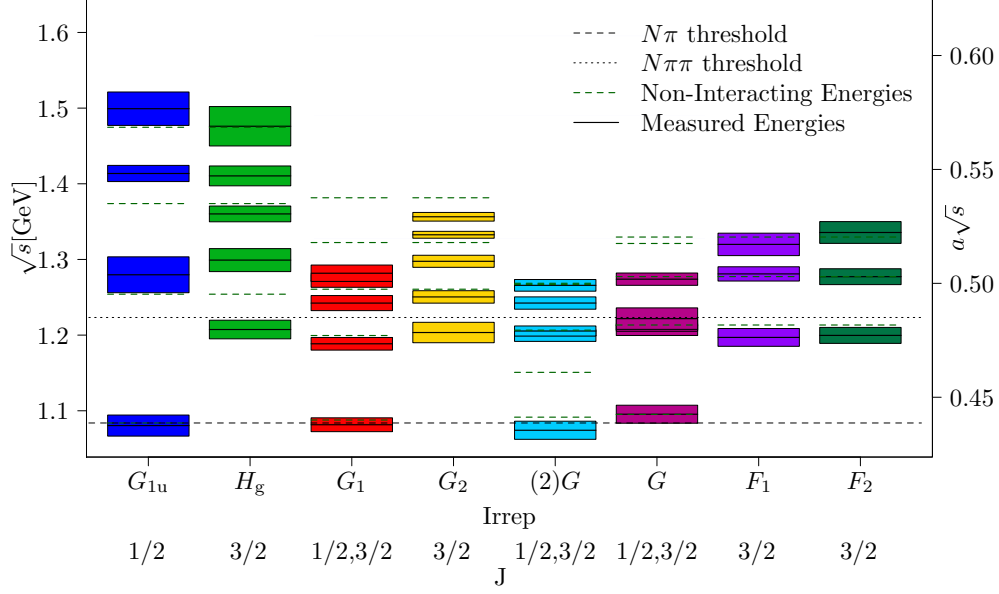


Figure 3: The invariant mass \sqrt{s} for the levels of the $\pi - N$ system in the rest and moving frames up to 3 lattice units of momentum and for all irreducible representations of the lattice rotation group. The $N\pi$ and $N\pi\pi$ thresholds are indicated by dashed and dotted horizontal lines respectively. The non-interacting energies for each irrep and frame is indicated by bold dashed horizontal segment.

where M^Λ is the finite volume Lüscher function[14], $\delta_{J\ell}$ is the infinite volume scattering phase shift for total angular momentum J and orbital angular momentum ℓ , and n is the occurrence of the irreducible representation Λ . We parameterize the energy dependence of the infinite volume phase shift. In this work, we use the s and p -wave phase shift parameterized by a constant scattering length and a Breit-Wigner type of resonance, respectively.

$$\cot \delta_{\frac{1}{2}0}(s) = a_0 q_{\text{cmf}}(s), \quad q_{\text{cmf}}^2(s) = \frac{(s - M_N^2 - M_\pi^2)^2 - 4M_N^2 M_\pi^2}{4s} \quad (6)$$

$$\tan \delta_{\frac{3}{2}1}(s) = \frac{\sqrt{s} \Gamma(\Gamma_R, M_R, s)}{M_R^2 - s}, \quad \Gamma(\Gamma_R, M_R, s) = \Gamma_R \left(\frac{q_{\text{cmf}}(s)}{q_{\text{cmf}}(M_R^2)} \right)^3 \frac{M_R^2}{s} \quad (7)$$

To obtain the Lüscher prediction of the finite volume spectrum for a given resonance mass (M_R) and resonance width (Γ_R) we solve the LQC eq. (5) numerically. In the angular-momentum we truncate the LQC by $\ell = 1$, and consider only the two partial waves in eq. (6) and (7). To estimate the effect of the truncation in ℓ we determine the roots of LQC using physical parameters for s and p -wave and including $\ell = 3$ ($\ell = 2$) in the center-off-mass frame (moving frames). We use $\tan(\delta_{J\ell}) = (a_\ell q_{\text{cmf}})^{2\ell+1}$ to parameterize higher partial waves with $a_\ell = -0.001 \frac{1}{\text{MeV}^{2\ell+1}}$. We show the comparison of this test with our numerically determined spectrum on Fig. 4. These results show that the third energy level in the Hg and already the second energy level in the G2 irrep cannot be explained solely using the dominant p -wave approximation and thus are not expected to play a role in the

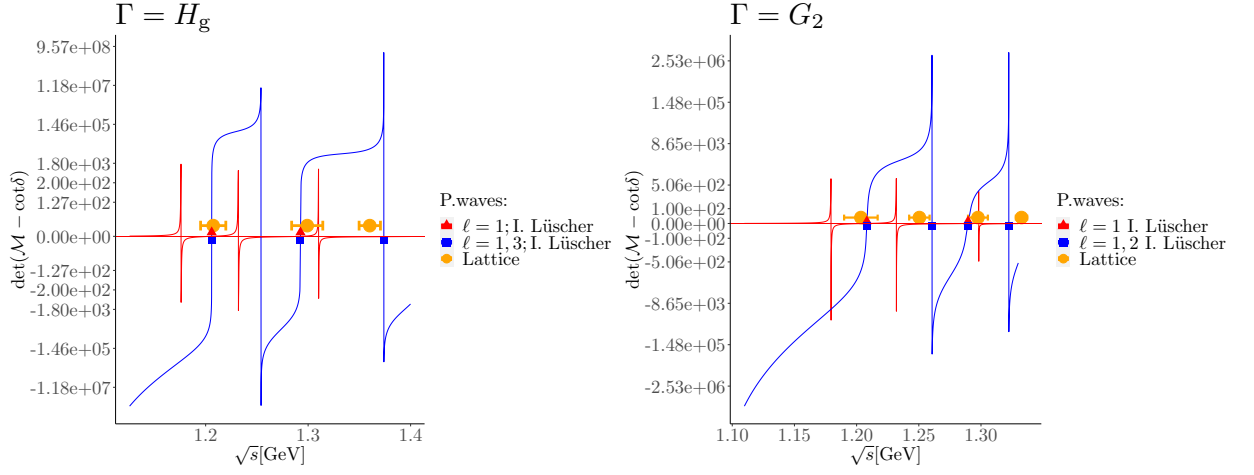


Figure 4: LQC for irrep H_g (left) and G_2 (right) using partial waves $\ell = 1, 2, 3$. LQC with $\ell = 1$ ($\ell \geq 1$) shown by continuous red (blue) curve and corresponding roots with triangle (rectangle) symbols. Lattice results are shown with big yellow circle with error bar. Red triangles and blue circles are obtained using the inverse Lüscher method as described the text in detail.

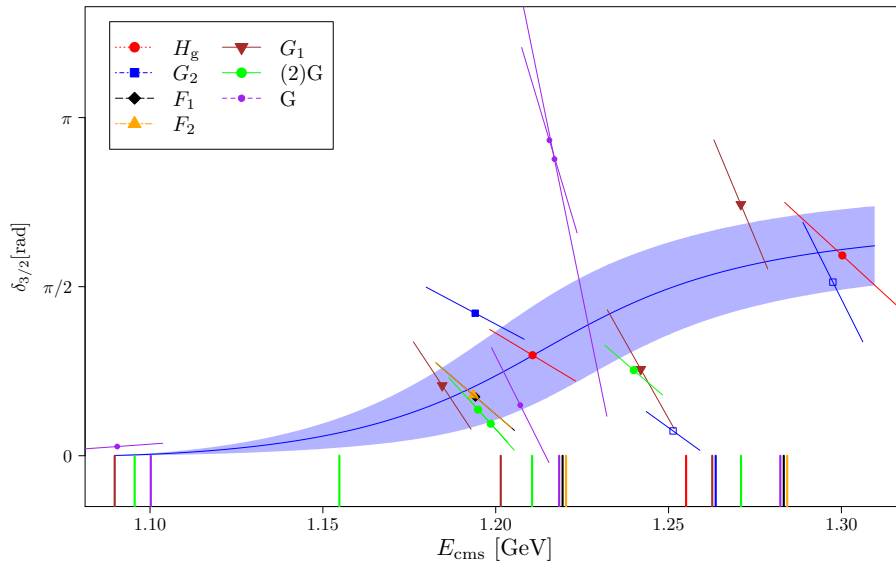


Figure 5: $I = 3/2$ phase shift of the Δ resonance. Errors are determined using jackknife resampling. At the bottom of the plot with thin vertical lines we indicate the non-interacting energies.

description of the resonance. For this reason we omit them from the final analysis. The parameters of the Δ resonance are determined through a non-linear fit of the energy levels to the finite volume spectrum obtained by the LQC-s. For the parameters of the resonance we obtain $M_R = 1255(25)$ MeV, $\Gamma_R = 140(120)$ MeV and for the s -wave scattering length $a_0 = -0.0016(6)\text{MeV}^{-1}$ from the fit with an overall $\chi^2/\text{dof.} = 0.88$. We show the fitted phase-shift curve together with the computed phase-shifts for the energy levels in Fig. 5. The uncertainty band on the phase-shift curve is determined using jackknife resampling.

5. Conclusions

Our presented analysis is the first numerical resonance calculation at the physical point in the meson-baryon sector. We determined the parameters of the Delta resonance using Lüscher's method and find

$$M_R = 1255(25) \text{ MeV}, \quad \Gamma_R = 140(120) \text{ MeV} \quad (m_\pi = 139.43(9) \text{ MeV}) \quad (8)$$

compared to the experimentally determined values of $M_R^{\text{exp}} = 1232$ MeV and $\Gamma_R^{\text{exp}} = 120$ MeV. Our analysis is barely sensitive to the width of the resonance. Our future plans include the determination of the scattering length and investigation of the $I = 1/2$ channel as well, in order to determine the σ -term.

6. Acknowledgment

We would like to thank all members of ETMC for their constant and pleasant collaboration. The project is supported by PRACE under project ‘‘The $N\pi$ system using twisted mass fermions at the physical point’’ (pr79), the measurements are done on the Piz-Daint cluster at CSCS. KH is supported by the Cyprus Research Promotion foundation under contract number POST-DOC/0718/0100 and EuroCC project funded by the Deputy Ministry of Research, Innovation and Digital Policy and Cyprus The Research and Innovation Foundation and the European High-Performance Computing Joint Undertaking (JU) under grant agreement No 951732. The JU receives support from the European Union's Horizon 2020 research and innovation program. FP acknowledges financial support from the Cyprus Research and Innovation Foundation under project ‘‘NextQCD’’, contract no. EXCELLENCE/0918/0129. MP gratefully acknowledges support by the Sino-German collaborative research center CRC-110. The open source software packages QUDA [15–17], R [18, 19] have been used.

References

- [1] L. Maiani and M. Testa, Phys. Lett. B **245**, 585-590 (1990) doi:10.1016/0370-2693(90)90695-3
- [2] M. Luscher, Nucl. Phys. B **354**, 531-578 (1991) doi:10.1016/0550-3213(91)90366-6
- [3] M. Werner *et al.* [Extended Twisted Mass], Eur. Phys. J. A **56**, no.2, 61 (2020) doi:10.1140/epja/s10050-020-00057-4 [arXiv:1907.01237 [hep-lat]].
- [4] Y. Akahoshi, S. Aoki and T. Doi, Phys. Rev. D **104**, no.5, 054510 (2021) doi:10.1103/PhysRevD.104.054510 [arXiv:2106.08175 [hep-lat]].

- [5] C. Andersen, J. Bulava, B. Hörz and C. Morningstar, Nucl. Phys. B **939**, 145-173 (2019) doi:10.1016/j.nuclphysb.2018.12.018 [arXiv:1808.05007 [hep-lat]].
- [6] D. Guo, A. Alexandru, R. Molina and M. Döring, Phys. Rev. D **94**, no.3, 034501 (2016) doi:10.1103/PhysRevD.94.034501 [arXiv:1605.03993 [hep-lat]].
- [7] M. Fischer *et al.* [Extended Twisted Mass and ETM], Phys. Lett. B **819**, 136449 (2021) doi:10.1016/j.physletb.2021.136449 [arXiv:2006.13805 [hep-lat]].
- [8] A. R. Raduta, Phys. Lett. B **814**, 136070 (2021) doi:10.1016/j.physletb.2021.136070 [arXiv:2101.03718 [nucl-th]].
- [9] C. McNeile *et al.* [UKQCD], Phys. Rev. D **65**, 094505 (2002) doi:10.1103/PhysRevD.65.094505 [arXiv:hep-lat/0201006 [hep-lat]].
- [10] C. Alexandrou, S. Bacchio, P. Charalambous, P. Dimopoulos, J. Finkenrath, R. Frezzotti, K. Hadjiyiannakou, K. Jansen, G. Koutsou and B. Kostrzewa, *et al.* Phys. Rev. D **98**, no.5, 054518 (2018) doi:10.1103/PhysRevD.98.054518 [arXiv:1807.00495 [hep-lat]].
- [11] M. T. Hansen and S. R. Sharpe, Ann. Rev. Nucl. Part. Sci. **69**, 65-107 (2019) doi:10.1146/annurev-nucl-101918-023723 [arXiv:1901.00483 [hep-lat]].
- [12] The SAID website allows access to the inelasticities in all the partial waves of the pion nucleon scattering. Results can be obtained from: <http://gwdac.phys.gwu.edu>.
- [13] G. Silvi, S. Paul, C. Alexandrou, S. Krieg, L. Leskovec, S. Meinel, J. Negele, M. Petschlies, A. Pochinsky and G. Rendon, *et al.* Phys. Rev. D **103**, no.9, 094508 (2021) doi:10.1103/PhysRevD.103.094508 [arXiv:2101.00689 [hep-lat]].
- [14] M. Gockeler, R. Horsley, M. Lage, U. G. Meissner, P. E. L. Rakow, A. Rusetsky, G. Schierholz and J. M. Zanotti, Phys. Rev. D **86**, 094513 (2012) doi:10.1103/PhysRevD.86.094513 [arXiv:1206.4141 [hep-lat]].
- [15] M. A. Clark, R. Babich, K. Barros, R. C. Brower and C. Rebbi, Comput. Phys. Commun. **181**, 1517-1528 (2010) doi:10.1016/j.cpc.2010.05.002 [arXiv:0911.3191 [hep-lat]]. [16]
- [16] M. A. Clark, B. Joó, A. Strelchenko, M. Cheng, A. Gambhir and R. Brower, [arXiv:1612.07873 [hep-lat]].
- [17] R. Babich, M. A. Clark, B. Joo, G. Shi, R. C. Brower and S. Gottlieb, doi:10.1145/2063384.2063478 [arXiv:1109.2935 [hep-lat]].
- [18] R: A Language and Environment for Statistical Computing, R Core Team <https://www.R-project.org/>
- [19] <https://github.com/HISKP-LQCD/hadron>, B. Kostrzewa and J. Ostmeyer, M. Ueding and C. Urbach